Journal of Power Sources 245 (2014) 164–170

Contents lists available at SciVerse ScienceDirect

Journal of Power Sources

journal homepage: www.elsevier.com/locate/jpowsour

Polarization characteristics of liquid antimony anode with smooth single-crystal solid oxide electrolyte

Hongjian Wang, Yixiang Shi*, Ningsheng Cai

Key Laboratory for Thermal Science and Power Engineering of Ministry of Education, Department of Thermal Engineering, Tsinghua University, Beijing 100084, China

HIGHLIGHTS

- Smooth electrolyte for intrinsic reaction kinetics.
- Polarization separation of liquid antimony anode.
- Sb_2O_3 framework for enhancing electrochemical oxidations.
- Polarization reduction by tuning Sb/Sb_2O3 ratio.

ARTICLE INFO

Article history:
Received 25 April 2013
Received in revised form
19 June 2013
Accepted 23 June 2013
Available online 1 July 2013

Keywords:
Liquid metal electrode
Antimony
Smooth electrolyte
Single crystal
Liquid ion conductor
Performance

ABSTRACT

A liquid antimony (Sb) anode is examined at 1073 K in solid oxide fuel cells with single-crystal yttria-stabilized zirconia (YSZ) electrolytes. Cells featuring a smooth electrolyte surface (Sa = 0.69 nm) are operated under "battery" mode with dry Ar flow in the anode chamber to characterize the electrochemical oxidation of the metals by oxygen ions while avoiding the effects of the electrolyte surface morphology. The intrinsic anode polarization of the liquid Sb anode is obtained, revealing that the Sb anode polarization was the main cause of performance loss. Because liquid Sb_2O_3 can transfer oxygen ions, the reaction product Sb_2O_3 decreases the anode polarization and enhances the performance by increasing the effective reaction interface. The liquid three-dimensional electrode is formed by discharging. The anode polarization can be reduced by changing the ratio of Sb and Sb_2O_3 in the anode. Using 50% Sb + 50% Sb_2O_3 as the anode, the anode resistance is reduced to 0.8 Ω cm^2, which is comparable to typical porous solid anodes.

1. Introduction

Liquid metal anode solid oxide fuel cells (LMA-SOFCs) are a clean, efficient, and competitive power generation technology for converting the chemical energy of various types of fuel into electricity. In this technology, oxygen from the solid electrolyte is transferred to the liquid metal to form the metal oxide, and the metal oxide can later be reduced by the fuel [1–6].

In past several years, a number of liquid metals have been studied for use as LMA-SOFC anodes. General electric first proposed the liquid Fe anode [7] for high-temperature carbon electrochemical conversion. Jacob et al. [8] used a liquid Cu anode in an LMA-SOFC. Cell Tech Co. developed the liquid tin anode solid oxide fuel cell to lower the cell operating temperature [5,9–13] However, the cell performance is often limited by the formation of an oxide film at the electrolyte interface. The anode polarization loss from the liquid Sn increased dramatically after cell operation, even under a fairly low current. Gorte et al. [14,15] systematically analyzed the electrochemical oxidation performance characteristics of Sn, Bi, In, Pb, and Sb. The cell polarization curves with liquid Sn, In, and Pb operating at 700–800 °C show typical limiting behavior due to the oxide layer formation with low oxygen ion conductivity. For the liquid Bi anode, a Bi_2O_3 oxide layer can also be formed, but its oxygen ion conductivity is relatively high. The liquid Sb anode has shown excellent performance for use in both battery mode for Sb electrochemical reaction with oxygen ions and carbon fuel mode. In one aspect, both Sb and Sb_2O_3 are liquids at typical SOFC operating temperatures, which is beneficial for the transportation of Sb towards the reaction active sites and the transportation of Sb_2O_3 away from the reaction active sites. In

* Corresponding author. Tel./fax: +86 10 62789955.
E-mail address: shyx@tsinghua.edu.cn (Y. Shi).

0378-7753/$ – see front matter © 2013 Elsevier B.V. All rights reserved.
http://dx.doi.org/10.1016/j.jpowsour.2013.06.125

addition, the liquid Sb_2O_3 is able to conduct oxygen ions with a conductivity of 0.0792 S cm^{-1} at 828 °C [16], which is of the same order of magnitude as the oxygen ion conductivity of yttria-stabilized zirconia (YSZ). Thus, except for the electrochemical oxidation of liquid Sb metal at the electrode/electrolyte interface, as occurs for other liquid metal anodes, liquid Sb can be electrochemically oxidized at the interface between the liquid Sb_2O_3 and liquid Sb phases. This mechanism may extend the electrochemically active area, which is closely related to cell polarization.

Based on the above discussion, the liquid Sb anode is a promising choice for use in a novel liquid metal anode fuel cell. However, the performance of liquid Sb anodes is still limited for multiple reasons, including the mechanism of charge transfer between the liquid electrode and electrolyte surface and the low electrochemical activity of the electrodes. Thus, it is important to understand the performance characteristics of the liquid Sb/electrolyte interface to improve the performance of these anodes.

Many studies have focused on the cell performance characteristics using a liquid Sb anode and novel prototype design development, especially the liquid Sb electrochemical oxidation and the reaction between liquid Sb_2O_3 and solid carbon [17–20]. However, most of the experimental characterizations of liquid Sb anode fuel cells in the literature have used commercially or self-prepared electrolyte layers with different surface roughness. The morphology of the electrode surface significantly affects the liquid metal electrochemical reaction characteristics, and the intrinsic electrochemical reaction rates are obfuscated by interface interactions and transport in rough porous anodes. In addition, the effects of the surface roughness on the cell couple with the effects of the Sb/Sb_2O_3 electrochemically active interface variation due to the composition variation of the liquid metal anode and make the transport and reaction processes within the liquid electrode more complex.

In this study, a liquid Sb anode solid oxide fuel cell is fabricated on a smooth single-crystal YSZ electrolyte substrate with a porous Pt cathode to investigate the intrinsic reacting kinetics of the electrochemical oxidation of liquid Sb. Polarization curves and electrochemical impedance spectroscopy (EIS) are used to evaluate the cell performance. The polarization of each cell component (anodic, cathodic, and electrolyte) is determined from specific experiments using a symmetric cell for polarization curves and EIS measurements. The discharge curves are used to analyze the effect of the reactant consumption and product accumulation on the cell performance. Scanning electron microscopy (SEM) is used to characterize the liquid Sb and electrolyte interface before and after the testing, and a novel reaction mechanism for liquid Sb electrochemical oxidation processes is proposed and discussed.

2. Experimental

2.1. Liquid Sb fuel cell preparation

A 25-mm diameter single-crystal smooth YSZ substrate with 13 mol% Y_2O_3 (<100> crystal orientation, Hefei Kejing Materials Technology Co., Ltd., China) was used as the electrolyte. The roughness of the electrolyte surface Ra is maintained at 0.69 nm, which is polished by chemical method. And the thickness of the electrolyte is 500 μm. The cathode was prepared from platinum paste (MC-Pt100, Grikin Advanced Materials Co., Ltd., China) by screen printing. The Pt paste layer was dried at 100 °C in air for 15 min. The calcination temperature for the cathode composite was set at 800 °C. Fig. 1a shows the surface morphology of the YSZ single crystal obtained by scanning electronic microscopy (SEM) (JSM-6460, JEOL, Japan), and Fig. 1b shows the YSZ surface roughness obtained by 3D profilometry (Phase Shift MicroXAM-3D, AEP Technology, USA).

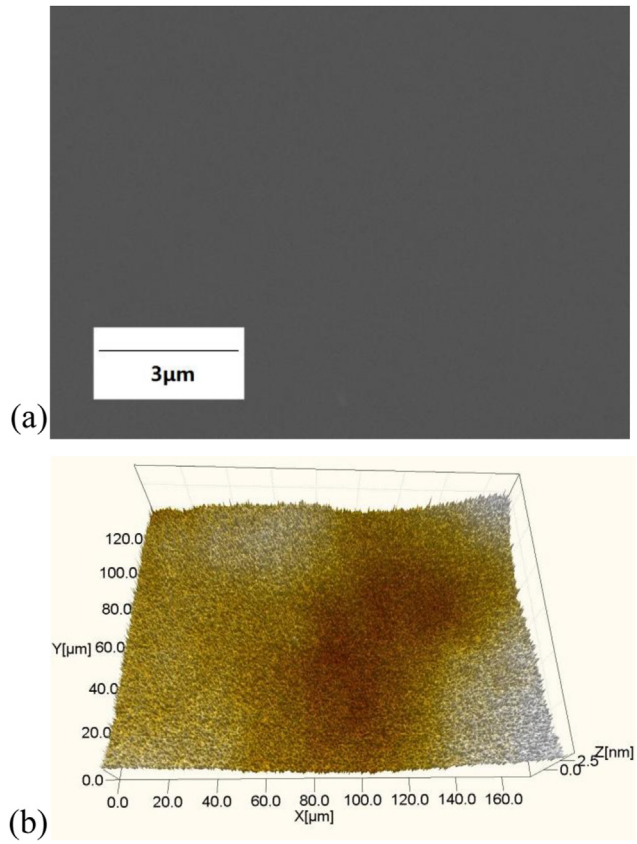

Fig. 1. Surface morphology characteristics of single-crystal YSZ electrolyte: (a) SEM images, (b) 3D profilometer images.

The cell was placed on the end of an alumina tube. An alumina plate was pressed to the button cell and fixed to three springs. A sealing glass ring was placed between the alumina tube and the button cell. On the cathode side, a platinum mesh was used as the current collector. On the anode side, a $Ni_{20}Cr_{80}$ ring was used as a current collector and to hold the antimony metal electrode above the electrolyte. The alumina tube was then set vertically to keep the liquid metal in contact with the single-crystal YSZ electrolyte. The antimony metal powder and carbon fuel powder can be added into the anode chamber during the cell operation by mounting the alumina tube. In this study, 2.0 g of antimony (99.5%, Sinopharm Chemical Reagent Co., Ltd., China) was added on top of the electrolyte. The thickness of the liquid metal anode should be approximately 1.5 mm according to an estimate based on the inner diameter of the current collector ring (16 mm) and the density of the liquid Sb at 800 °C (6.34 g cm^{-3}) [21].

2.2. Experimental testing setup

A liquid Sb anode fuel cell experimental testing setup was constructed for cell performance testing, as shown in Fig. 2.

The polarization curves were measured by the four-probe method using an electrochemical workstation (IM6ex, Zahner-Elektrik GmbH, Germany). Electrochemical impedance spectroscopy (EIS) was performed with an amplitude of 20 mV from 0.1 Hz to 100 kHz. The ohm resistance of the cell was estimated from the high-frequency intercept of the impedance curve. The measurements were initiated 30 min after the temperature of the system had stabilized. A K-type thermal couple was used to measure the temperature next to the button cell. The Ar gas for the anode

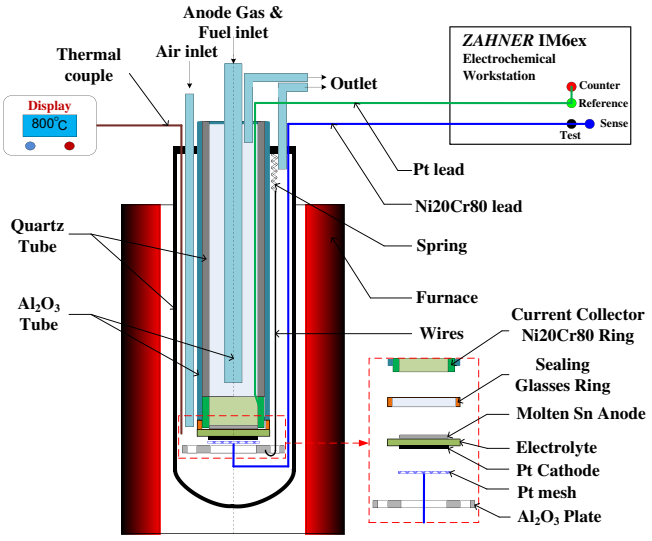

Fig. 2. Liquid Sb fuel cell testing setup.

chamber and the air for the cathode chamber are controlled by mass flow controllers.

During the tests, the button cell was heated from room temperature to 800 °C over 10 h with Ar shielding gas at a flow rate of 35 mL min^{-1} for both the anode and cathode chambers. The platinum paste was sintered for 30 min at 800 °C. The Ar gas flow rate in the anode was then increased to 50 mL min^{-1}, and the cathode gas was switched to air at 200 mL min^{-1}. Next, 2.0 g of Sb powder was added into the anode chamber through the alumina tube. During the cell performance testing process, the total flow rate of the anode gas was maintained at 50 mL min^{-1}, and the total flow rate of the cathode gas was maintained at 200 mL min^{-1}. After the cell tests, the cell surface and cross-section and the elemental distribution were characterized by SEM and EDS (energy dispersive spectrometry) using an electron probe microanalyzer (JSM-6460, JEOL, Japan).

2.3. Experimental characterization of the polarization of each cell component

To determine each polarization loss for the liquid Sb anode fuel cell, a symmetric cell was used to estimate the cell cathode polarization. The symmetric cathode was printed in the same way as described previously for the single-button cell on a single-crystal YSZ substrate with the same surface morphology of the liquid Sb fuel cell cathode in both sides. The total ohmic resistance was determined by EIS tests on the symmetric cell from the high-frequency intercept of the impedance curve. The cathodic polarization was determined by subtracting the ohmic polarization from the measured polarization and then dividing by two. The anodic polarization was then estimated by subtracting the ohmic polarization, cathodic polarization, and leak overpotential from the total polarization of the single cell. The symmetric cell used for polarization measurements should be carefully prepared to make sure that the cathodes in the symmetric cell and the single-button cell are identical. Based on high-frequency EIS measurements, considering that the electrodes are good conductors, it is reasonable to assume that the resistance thus determined (high-frequency intercept of the impedance curves) include the contact and electrolyte ohmic resistances. The polarization due to contact and electrolyte resistances was then calculated from the resistance determined by EIS measurements.

3. Results and discussion

3.1. Liquid Sb anode performance in battery mode

Fig. 2 shows the IV curves and EIS spectra of the liquid Sb anode fuel cell in battery mode. It can be observed that the open circuit voltage (OCV) of the liquid Sb anode was 0.750 V, which agreed well with the theoretical OCV of 0.738 V (supposing that the activity of liquid Sb and Sb_2O_3 are both equal to 1) at 1073 K. The current density was measured by decreasing the cell operating voltage from the OCV at the rate of 10 mV s^{-1}, which is referred to as the forward IV curve in this study. When the cell potential reached zero, the potential was ramped up at a rate of 10 mV s^{-1} to the OCV, which is referred to as the backward IV curve in this study. The IV curve shows that when the cell working voltage was below 0.68 V, the forward-scanning current density was lower than the backward-scanning current density at the same working voltage. The maximum voltage difference between the forward and backward current density was approximately 91 A m^{-2} at 0.4 V. When the cell voltage was below 0.4 V, the forward IV curve was linear with a slope of 20 Ω cm^2, which demonstrates that the area-specific resistance (ASR) of the cell was independent of current density in this region. However, for the backward IV curve, when the working voltage was above 0.4 V, the backward IV curve was linear with a slope of 14 Ω cm^2, which demonstrates that the cell performance improves during the cell discharging processes. It should be noted that the OCV decreases from 0.75 V to 0.70 V for the backward-scanning IV curve, which is most likely due to the accumulation of the reacting product Sb_2O_3 at the interface of the liquid anode and electrolyte.

The Nyquist plot of the EIS spectra in Fig. 3b shows that the ohm resistance remained almost constant, increasing only slightly from 4.15 Ω to 4.20 Ω. In contrast, the non-ohmic portion of the cell impedance was halved, decreasing from approximately 20 Ω–10 Ω.

In Fig. 3a, the anode, cathode, and ohmic polarizations of the cell were also determined. The polarization of the Pt cathode used in this study was characterized separately using a symmetrical cell experimental setup. The cathode polarization is compared with the anode and ohmic polarizations. It is also noteworthy that the cell performance in Fig. 3 was achieved using a thick single-crystal electrolyte-supported button cell. If the electrolyte thickness is further reduced using a cathode-supported cell or novel materials, the electrolyte polarization will be greatly reduced. However, it can be concluded that the largest proportion of the polarization resistance in the impedance of the liquid Sb anode SOFC is due to the liquid anode polarization. It can also be deduced that the ohmic polarization and cathode polarization were the same in both the forward- and backward-scanning IV curves, and the anode polarization of the backward IV testing was only half that of the forward anode polarization. The anode polarization reduction after discharging may be ascribed to the production of liquid Sb_2O_3 at the liquid Sb/electrolyte interface, which can enhance the oxygen ion transportation to liquid Sb and effectively extend the electrochemical reaction area by forming a liquid Sb and Sb_2O_3 interface.

Next, two additional forward–backward IV scanning cycles were tested, in which the OCV remained almost constant at 0.70 V. The forward IV curve improved during the IV curve testing, and the limiting current density increased from 320 to 338 A m^{-2}. All of the backward IV curves were nearly the same and better than the forward IV curves. The EIS spectra shows that the ohmic polarization was almost the same for different cycles, and the non-ohmic polarization further decreased after the 2nd and 3rd cycling tests. Because the cathode polarization remained almost the same, the performance improvement was mainly attributed to the decrease in the anode polarization. This finding further suggests that the

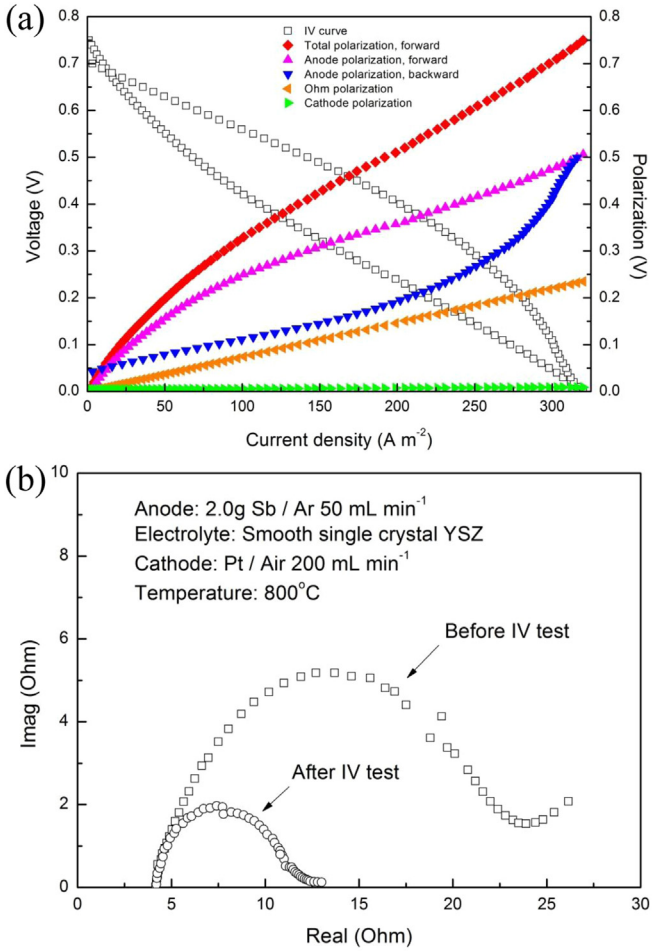

Fig. 3. Performance of the liquid Sb anode fuel cell in battery mode: (a) polarization curves, (b) EIS curve.

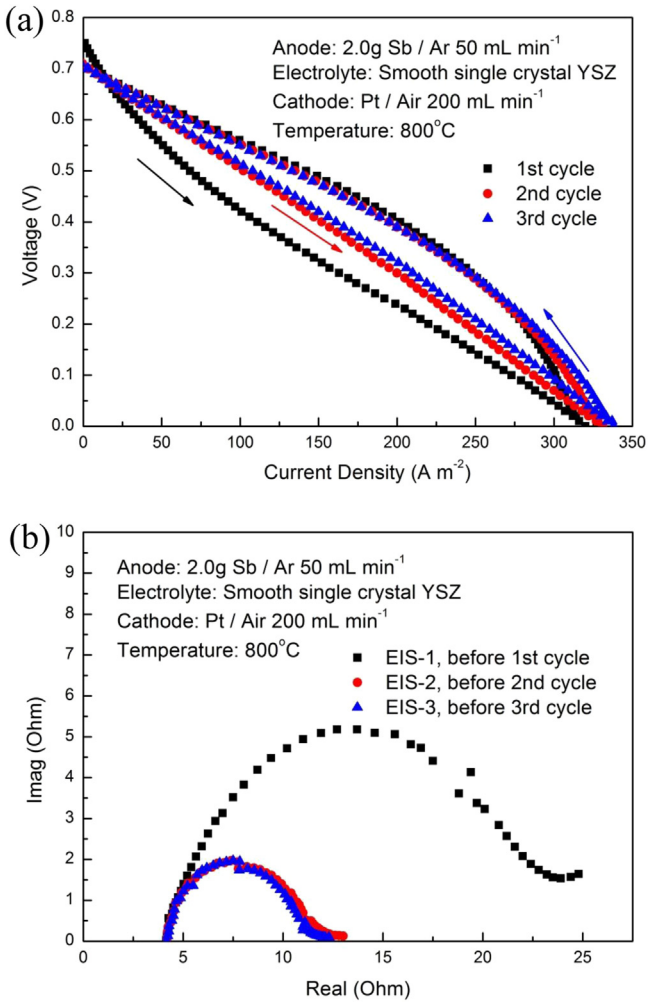

Fig. 4. Continuous IV testing of the liquid Sb anode DCFC in battery mode: (a) IV curves, (b) EIS spectra.

production of Sb_2O_3 at the beginning of the cell discharge process can improve the anode performance.

3.2. Performance variation during cell discharging

To further study the cell performance variations due to the variations of Sb and Sb_2O_3 ratio, we discharged the liquid Sb anode fuel cell in the battery mode at constant voltage 0.3 V, as shown in Fig. 5. The results indicated that the current density of the cell increased gradually from 184 to 297 A m^{-2} after discharging for approximately 1730 s. After the current density remained at 297 A m^{-2} for 500 s, it began to decrease and then plateau at approximately 290 A m^{-2} for 1000 s, after which the current density decreased again. Suppose that only 50% of the 2.0 g Sb converts into Sb_2O_3, and the cell works at constant current density 300 A m^{-2}, according to the charge conservation it can discharged for 12.45 h. Further, by integration using the D-value method, the total charge was 82.7 C during the 1 h discharge as shown in Fig. 5. According to the charge conservation equation, the consumed Sb was only 0.0347 g. So the liquid Sb was not used up during testing. The performance fading was mainly due the product Sb_2O_3 accumulation, which did not break away from the interface between the liquid Sb anode and YSZ electrolyte due to surface tension and viscosity. In fact, there were several ways to avoid the cell performance fading: (a) stirring the liquid Sb to promote the Sb_2O_3 convection in the liquid Sb which has been applied to the liquid Sb anode SOFC [14,18]. However, this method can only put off the performance fading, as the cell discharge for longer time, more and more Sb are converted into Sb_2O_3 and no enough Sb is provided for discharge, then the cell performance decreases. In this condition,

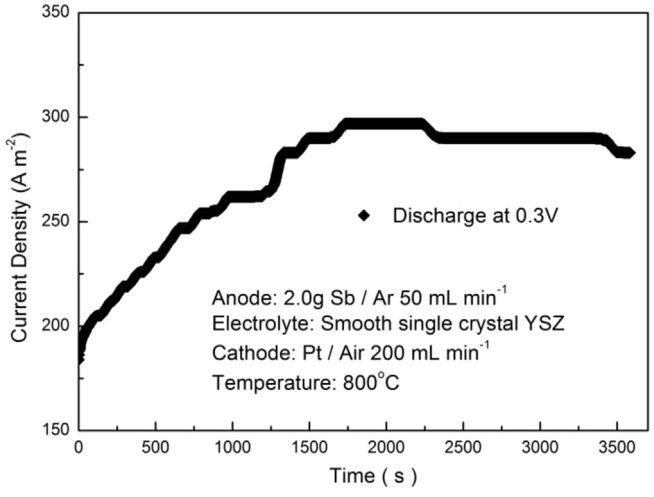

Fig. 5. Discharge performance at a constant working voltage of 0.3 V for 1 h.

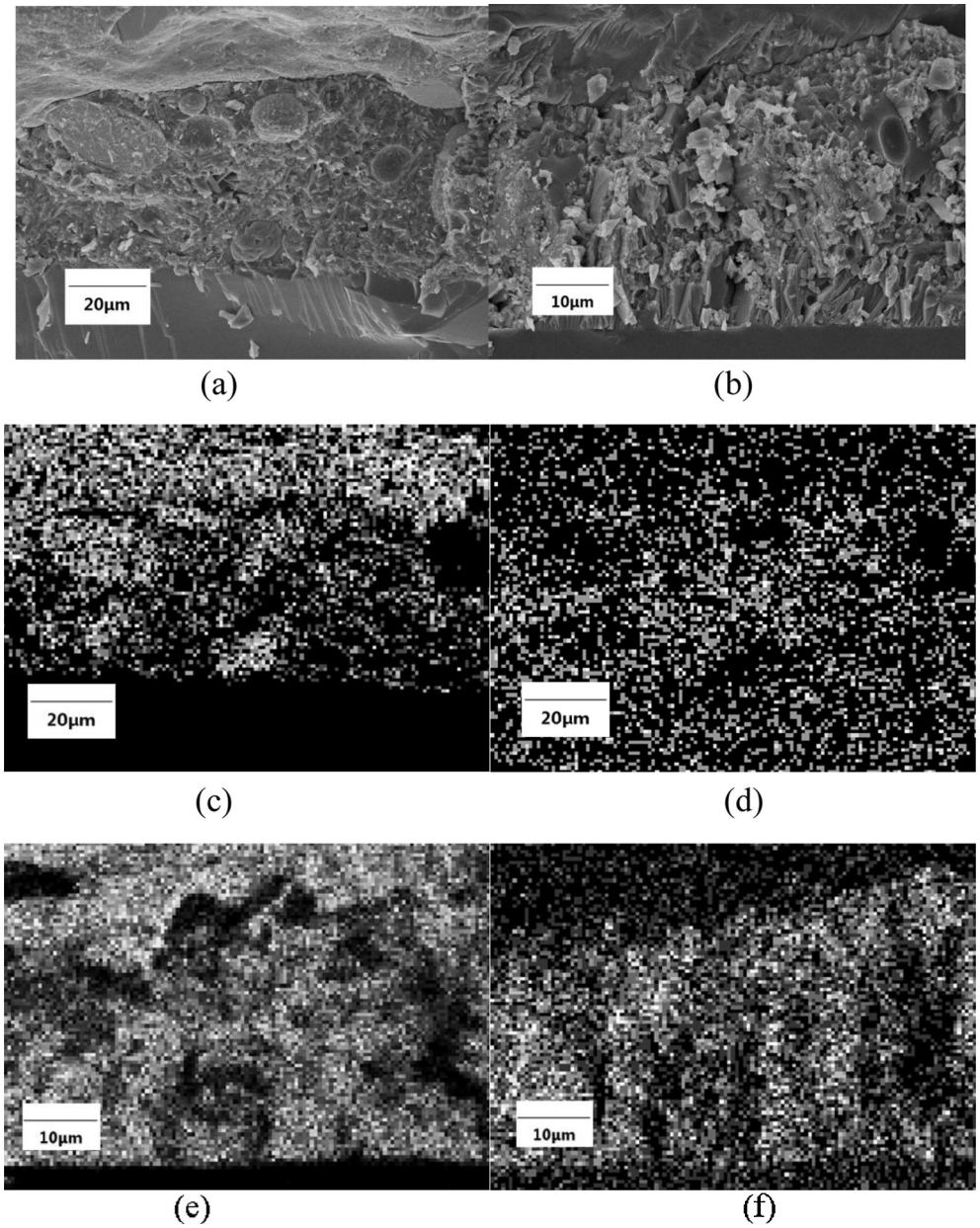

Fig. 6. SEM image and Sb/oxygen distribution of the interface between the anode and electrolyte: (a) interface without discharge, (b) interface after discharge for 1 h, (c) Sb distribution without discharge (white dots denote Sb), (d) oxygen distribution without discharge (white dots denote oxygen), (e) Sb distribution after discharge for 1 h (white dots denote Sb), (f) oxygen distribution after discharge for 1 h (white dots denote oxygen).

fresh Sb need to be filled into the anode chamber and the product should be removed from the anode chamber. And Javadekar [18] proposed a system based on this concept. (b) When the fuel such as H_2, CO, CH_4 or carbon fuel is added into the anode chamber, the performance also can be regenerated by reducing the product Sb_2O_3 into Sb. Especially, the method using carbon fuel to reduce of Sb from its oxide is presently carried out on a commercial scale [22]. (c) It is also possible to regenerate Sb from Sb_2O_3 by electrolysis [18]. The liquid Sb anode SOFC can work at both fuel cell mode and electrolysis mode, which is more like a rechargeable battery in this case.

To observe the formation of Sb_2O_3 near the YSZ interface during the cell discharging processes, the same experiments as that shown in Fig. 4 without discharge and that shown in Fig. 5 with 1 h of discharge were performed. The cell was then cooled to room temperature, and the distribution of Sb_2O_3 near the Sb/YSZ electrolyte interface was characterized experimentally using SEM and EDX. In Fig. 6a, three layers can be observed at the section of the interface between the Sb anode and YSZ. The pure Sb layer is on the top, the YSZ layer is on the bottom, and Sb and Sb_2O_3 mixtures are in between. For the cell cross-section view after discharging, as shown in Fig. 6b, there were also three layers, just as in the cell cross-section view for the cell without discharge. The results indicated that the morphology of the Sb and Sb_2O_3 mixtures was quite different for the above two testing cases due to the differences in the ratio of Sb and Sb_2O_3. Fig. 6c and d shows that the Sb and oxygen distribution of the section shown in Fig. 6a, respectively. While, Fig. 6e and f shows that the Sb and oxygen distribution of the section shown in Fig. 6b, respectively. Obviously, there were many more grains and more Sb_2O_3 appeared for the cell after discharge. It

is very interesting that the Sb and oxygen distribution may form a three-dimensional conducting framework for oxygen ions and for the contacts between the metal electrode and metal oxide oxygen ion conductors, which would greatly decrease the anode polarization and increase the cell performance.

3.3. Proposed reaction mechanisms for the liquid Sb anode

Based on the above-reported performance characteristics of the liquid Sb anode, a schematic illustration of the plausible mechanism is presented in Fig. 7. In the initial state, liquid Sb was wetted on the extremely smooth surface of an YSZ single-crystal electrolyte, and the electrochemical reaction of Sb could only occur at the interface of liquid Sb and YSZ, which is labeled with red lines in Fig. 7 to denote the reaction boundary. After discharging for a relatively short period, liquid Sb_2O_3 product accumulated on the interface as bubbles, and the liquid Sb_2O_3 traveled from the Sb/YSZ interface to the liquid Sb anode surface. Because the liquid Sb_2O_3 can effectively transfer oxygen ions, the actual reaction area of Sb electrochemical oxidation increased greatly with the discharge. Under these conditions, the liquid phase three-dimensional mixed electronic-ionic conducting framework is formed. At the same time, the liquid Sb_2O_3 will diffuse into the liquid Sb and further decrease the anode polarization. After a longer discharging process, the liquid Sb_2O_3 product accumulation will increase the oxygen ion transport resistance and the effective reaction area between the electronic conductor and ionic conductor will decrease, deteriorating the cell performance.

3.4. Liquid Sb anode performance with 50% Sb with 50% Sb_2O_3

To further study the effects of the ratio of Sb to Sb_2O_3 on the liquid Sb anode performance, 50% Sb and 50% Sb_2O_3 (the total mass of Sb was 2 g) were used as the liquid anode. From Fig. 8a, it can be observed that when using the 50% Sb and 50% Sb_2O_3 mixture liquid anode, the current density of the backward-scanning *IV* curve was lower than that of the forward-scanning *IV* curve at the same working voltage. This phenomenon indicated that the production of Sb_2O_3 in this state did not substantially affect the cell performance, as the ratio of Sb and Sb_2O_3 near the anode/electrolyte interface remained almost stable during the polarization curve testing. Fig. 8b shows that the anode polarization with 50% Sb and 50% Sb_2O_3 was much lower than that of the anode with pure Sb. The proximate equivalent ASR for anode polarization can decrease from 18 Ω cm^2 to 2.2 Ω cm^2, which indicated that it was crucial to explore the detailed reaction mechanism near the anode/electrolyte interface in different local interface ratios of Sb and Sb_2O_3, which may guide the design of a novel liquid Sb anode with low anode polarization.

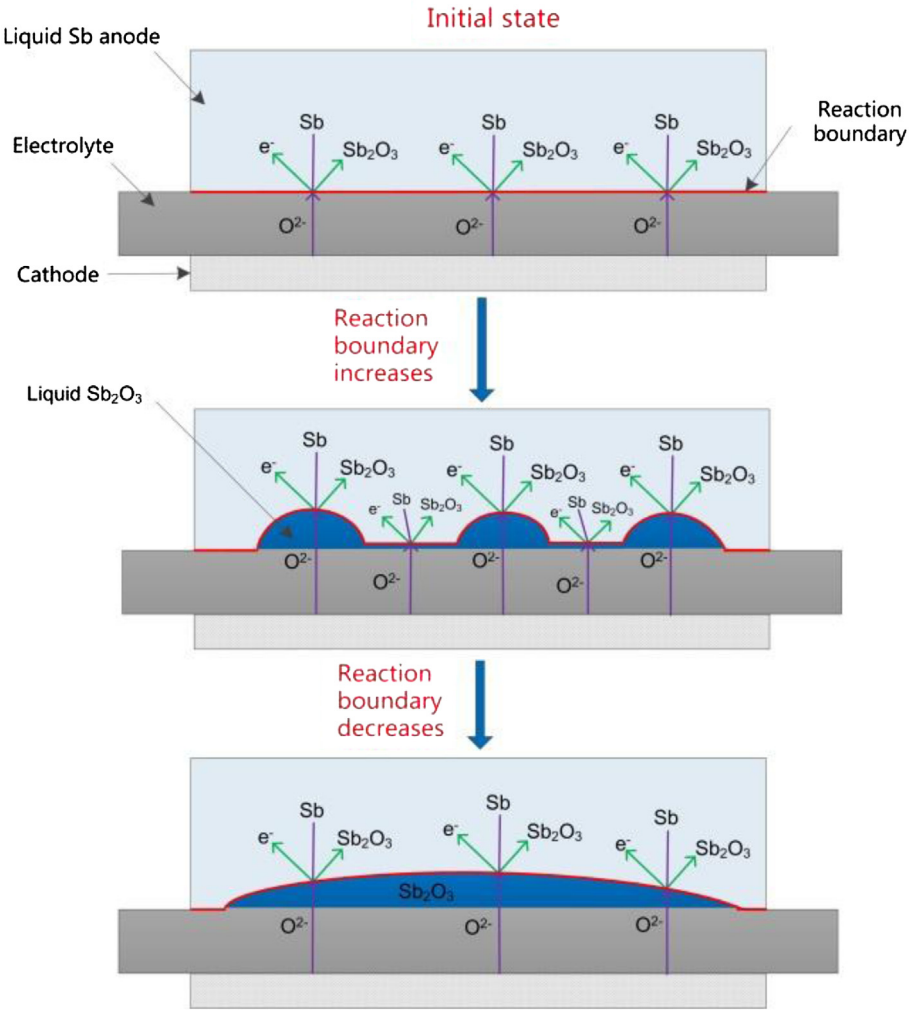

Fig. 7. Proposed reaction processes near the liquid Sb anode/electrolyte interface.

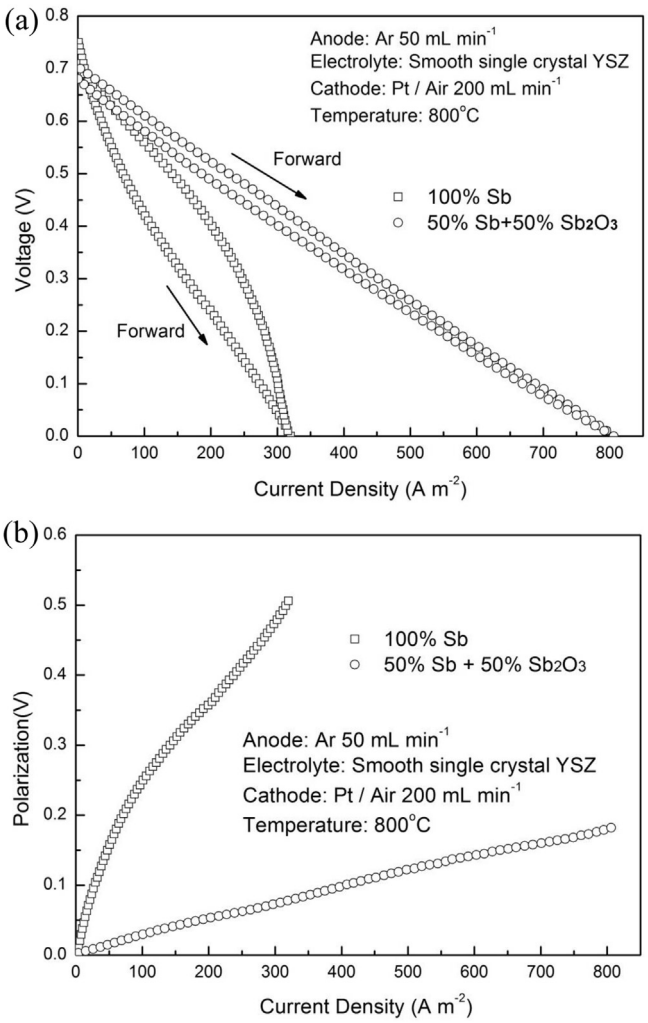

Fig. 8. Performance of the liquid Sb anode with different ratios of Sb and Sb_2O_3: (a) *IV* curves, (b) anode polarization.

4. Conclusions

A liquid Sb anode solid oxide fuel cell is fabricated on a smooth single-crystal YSZ electrolyte substrate with a porous Pt cathode to reveal the intrinsic reaction kinetics of the electrochemical oxidation of liquid Sb. The polarization of each cell component (anodic, cathodic, and electrolyte) is determined from specific experiments using a symmetric cell for polarization curves and EIS measurements.

The intrinsic anode polarization of the liquid Sb anode solid oxide fuel cell was obtained, and a plausible mechanism for the liquid Sb anode was proposed. It is suggested that the anode polarization can be effectively reduced by Sb_2O_3 production during Sb electrochemical processes in the initial operation of the pure liquid Sb anode, as well as by adjusting the ratio and distribution of Sb and Sb_2O_3. One possible explanation is the formation of the liquid three-dimensional electronic and ionic conducting framework, which could dramatically increase the effective contact area between the electronic conductor (liquid Sb) and ionic conductor (liquid Sb_2O_3 and electrolyte). The proximate equivalent ASR for anode polarization can be reduced from 18 Ω cm^2 to 2.2 Ω cm^2. Further effort should focus on exploring the detailed reaction mechanism near the anode/electrolyte interface, which may guide the design of a novel liquid Sb anode with low anode polarization.

Acknowledgments

This work was supported by the National Natural Science Foundation of China (51106085, 20776078) and the Seed Funding of Low Carbon Energy University Alliance.

References

[1] D.X. Cao, Y. Sun, G.L. Wang, J. Power Sources 167 (2007) 250–257.
[2] R.H. Wolk, S.M. Lux, S. Gelber, F.H. Holcomb, ERDC-CERL Fuel Cell Program Report (2007).
[3] T.M. Gur, J. Eletrochem. Soc. 157 (2010) B751–B759.
[4] S. Giddey, S.P.S. Badwal, A. Kulkarni, C. Munnings, Prog. Energ. Combust. 38 (2012) 360–399.
[5] T. Tao, Proceedings of Ninth International Symposium Solid Oxide Fuel Cells, vol. 1, 2005. pp. 353–62.
[6] A. Toleuova, V. Yufit, S. Simons, W.C. Maskell, D.J.L. Brett, J. Electrochem. Sci. Eng. 3 (2013) 91–105.
[7] E.T. William, et al. US Patent, 3138490, 1964.
[8] K.T. Jacob, ECS Trans. 35 (2011) 573–582.
[9] T. Tao, Direct Carbon Fuel Cell Workshop, Pittsburgh, PA, 2003.
[10] T. Tao, W. McPhee, M. Koslowske, J. Bentley, M. Slaney, L. Bateman, ECS Trans. 25 (2009) 1115–1124.
[11] R. Gemmen, H. Abernathy, K. Gerdes, M. Koslowske, W.A. McPhee, T. Tao, J. Am. Ceramic Soc. 5 (2010) 37–52.
[12] J.M. Bentley, Fuel Cell Seminar, San Antonio, Texas, 2010.
[13] W.A.G. McPhee, L. Bateman, M. Koslowske, M. Slaney, Z. Uzep, J. Bentley, T. Tao, J. Fuel Cell Sci. Technol. 8 (2011) 041007–041011.
[14] A. Jayakumar, S. Lee, A. Hornés, J.M. Vohs, R.J. Gorte, J. Eletrochem. Soc. 157 (2010) B365–B369.
[15] A. Jayakumar, J.M. Vohs, R.J. Gorte, Ind. Eng. Chem. Res. 49 (2010) 10,237–10,241.
[16] A.E.V. Arkel, E.A. Flood, Can. J. Chem. 31 (1953) 1009–1019.
[17] A. Jayakumar, R. Küngas, S. Roy, A. Javadekar, D.J. Buttrey, J.M. Vohs, R.J. Gorte, Energy Environ. Sci. 4 (2011) 4133–4137.
[18] A.D. Javadekar, Molten Metal Electrodes in Solid Oxide Fuel Cells. Doctor dissertation, University of Delaware, 2012.
[19] A. Javadekar, A. Jayakumar, R.J. Gorte, J.M. Vohs, D.J. Buttrey, J. Eletrochem. Soc. 159 (2012) A386–A389.
[20] A. Jayakumar, A. Javadekar, J. Gissinger, J.M. Vohs, G.W. Huber, R.J. Gort, J. AIChE (2012), http://dx.doi.org/10.1002/aic.13965 2012.
[21] D.J. Steinberg, Metall. Trans. 5 (1974) 1341–1343.
[22] J.A. DeCew, Metall. Chem. Eng. 16 (1917) 444–449.